JOURNAL OF VIROLOGY, Aug. 1981, p. 401-406
0022-538X/81/080401-06$02.00/0

Vol. 39, No. 2

Synthesis of Subgenomic mRNA's of Mouse Hepatitis Virus Is Initiated Independently: Evidence from UV Transcription Mapping

LIESBETH JACOBS, WILLY J. M. SPAAN, MARIAN C. HORZINEK, AND BERNARD A. M. VAN DER ZEIJST*

Institute of Virology, Veterinary Faculty, State University, 3508 TD Utrecht, The Netherlands

Received 23 February 1981/Accepted 27 April 1981

The target sizes of the templates for the synthesis of the genome-sized RNA and the six subgenomic RNAs found in cells infected with mouse hepatitis virus strain A59 were determined by UV transcription mapping. Infected Sac(−) cells were irradiated at 6 h postinfection, the time when virus-specific RNA synthesis starts to increase exponentially. The effect of increasing UV doses on the synthesis of the individual RNAs was determined by quantitation of these RNAs after separation by agarose gel electrophoresis. The UV target sizes calculated for the templates were almost identical to the physical sizes of the RNAs. The results of these experiments seem to exclude the possibility that the subgenomic RNAs are processed or spliced from a common precursor. The data are consistent with independent initiation of transcription on a genome-sized, negative-stranded template or on smaller templates.

Coronaviruses differ from other positive-stranded RNA viruses in that multiple subgenomic mRNA's are used for the synthesis of their proteins. As we have described before (7), seven virus-specific RNA species are synthesized in cells infected with mouse hepatitis virus strain A59 (MHV-A59). Their molecular weights are: 5.6×10^6 (RNA 1), 4×10^6 (RNA 2), 3×10^6 (RNA 3), 1.4×10^6 (RNA 4), 1.2×10^6 (RNA 5), 0.9×10^6 (RNA 6), and 0.6×10^6 (RNA 7). RNA 1 has the same size as the viral genome; both RNAs have identical RNase T_1 fingerprints (W. J. M. Spaan, unpublished data). All RNAs are polyadenylated and present in polyribosomes. A set of six virus-specified RNAs has been described by Stern and Kennedy (8) in cells infected with infectious bronchitis virus, an avian coronavirus. Comparison of RNase T_1 fingerprints of these RNA species has shown that they are from a nested set. The sequence of each RNA is contained within the sequences of all larger RNAs. All RNAs have a sequence in common which is localized at the 3′ end of the genome (8, 9).

Translation of MHV-A59 RNA species 3, 6, and 7 in *Xenopus laevis* oocytes yielded products that were immunoprecipitable with an antiserum raised against the viral structural proteins. The products comigrated with the intracellular precursor for the peplomeric protein (gp90/180/E2), with the smaller envelope protein (gp24/25.5/26.5/E1), and with the nucleocapsid protein (pp54/N), respectively (4). These data, together with those obtained by Siddell et al. for mouse hepatitis virus strain JHM (6) show that at least three RNA species are messengers for single primary protein products, presumably encoded by the unique 5′-terminal sequence of each mRNA (11).

In this paper, we want to answer the question of whether the multiple virus-specific RNAs found in MHV-A59-infected cells are derived by processing or splicing of larger precursor molecules, or whether they arise from independent transcription units. We used UV transcription mapping to approach this problem.

UV transcription mapping makes use of the fact that UV irradiation of RNA molecules induces uracil dimers (3). It is assumed that (i) the formation of one dimer is sufficient to stop transcription of an RNA chain at that point; (ii) repair is slow or absent; and (iii) the number of hits at a given dose rate will be proportional to the time of irradiation and to the length of the template (target size). The probability that a sequence is transcribed is identical to the probability that there are no UV lesions on the corresponding template between the promoter site and the end of the region coding for the sequence. The Poisson distribution applies, which may be expressed as $\ln(N_t/N_0) = -K \times T \times t$, where N_t is the rate of RNA synthesis after t seconds of irradiation, N_0 is the RNA synthesis in the unirradiated culture, T is the target size,

and K is a constant. UV transcription mapping has been applied successfully to determine the target sizes of transcription templates for a number of viral mRNA's (5).

MATERIALS AND METHODS

Cells and virus. Sac(−) cells were grown in Dulbecco modified Eagle medium (DMEM) supplemented with 10% fetal calf serum (FCS), penicillin (100 IU), and streptomycin (100 μg/ml). MHV-A59 obtained from the American Type Culture Collection was plaque purified twice, and virus stocks were prepared by infecting Sac(−) cells at a low multiplicity of infection as described previously (7). To obtain the high-titered virus stocks needed for infection of cells at a high multiplicity of infection, the virus was concentrated and purified. The plaque assay was also the same as that described before, with the exception that a different line of L-cells, obtained from F. Lehmann-Grube (Hamburg, West Germany), was used. With these cells, plaques could be read within 24 h.

Virus infection. Confluent 35-mm dishes containing about 2×10^6 Sac(−) cells were infected with 10 to 20 PFU per cell in an inoculum of 0.3 ml of DMEM-3% FCS. Mock infections were carried out with 0.3 ml of DMEM-3% FCS. Virus adsorption was continued for 1 h at 37°C with periodic gentle shaking of the dishes, the inoculum was removed, and 1 ml of DMEM-10% FCS was added.

Labeling of the virus-specific RNAs and UV irradiation of infected cells. At 5 h after infection, the medium was replaced by 1 ml of DMEM-10% FCS containing 1 μg of actinomycin D per ml, and at 6 h after infection, the medium was removed, and cultures were UV irradiated for various intervals at a dose rate of 50 erg s^{-1} mm^{-2}. A 30-W germicidal lamp at a distance of 50 cm was employed for this purpose. The dose rate was determined by using a model J225 Blak-Ray Ultraviolet meter (Ultraviolet Products, Inc., San Gabriel, Calif.). After irradiation, the cultures were incubated for 30 min in 1 ml of DMEM-10% FCS containing 100 μCi of [^{3}H]uridine and 1 μg of actinomycin D.

Isolation of virus-specific RNA from infected cells. At the end of the labeling period, the cells were washed with ice-cold phosphate-buffered saline and lysed with 0.4 ml of TES buffer (20 mM Tris-hydrochloride, 1 mM EDTA, 0.1 M NaCl, pH 7.4) containing 0.5% Triton X-100 and 0.5% 1,5-naphthalenedisulfonate·Na_2. After 10 min of incubation at 4°C, nuclei and cell debris were removed by centrifugation at 1,000 × g for 5 min at 4°C, and 0.35 ml of TES buffer containing 2% sodium dodecyl sulfate and 7 M urea (Aristar grade; BDH, Poole, England) was added to 0.35 ml of the supernatant, followed by the addition of 0.7 ml of redistilled phenol saturated with TES buffer and containing 0.1% 8-hydroxyquinoline at room temperature. The phases were separated by centrifugation (20 min, 10,000 × g), and RNA was precipitated from the aqueous phase by the addition of 2 volumes of ethanol and 1 M sodium acetate (pH 5.2) to a final concentration of 0.1 M. The mixture was kept at −20°C for at least 16 h, and the RNA was recovered by centrifugation at 10,000 × g for 20 min at 0°C (7).

Agarose gel electrophoresis of RNA. Denaturation of RNAs with glyoxal and dimethyl sulfoxide by a modification of the method of McMaster and Carmichael (2) and electrophoresis of RNAs in urea-containing 1% agarose gels followed by impregnation of the gels with En^{3}Hance (New England Nuclear Corp., Dreieich, West Germany) have been described previously (7). After fluorography of the dried gels, performed by exposure to preflashed Kodak XR or XS films at −70°C (1), the RNA bands were excised from the gel and dissolved by boiling in 0.5 ml of water for 10 min. After the addition of 4.5 ml of scintillation fluid (Emulsifier Scintillator 229, Packard Instrument Co., Rockville, Md.), the radioactivity was counted.

Counting of samples of radioactive RNA. Unless otherwise stated, samples were spotted on Whatman 3MM filter paper disks that were washed three times in 5% trichloroacetic acid, once in ether-ethanol, and once in ether before they were dried and counted.

RESULTS

Effect of UV irradiation on the total synthesis of MHV-A59-specific RNAs. We chose to UV irradiate infected cells at 6 h postinfection, at which time there is an exponential increase in virus-specific RNA synthesis; all of the virus-specific RNA made in infected cells between 6 and 8 h postinfection is present in polyribosomes or nucleoprotein particles (7). We assumed that by this time most of the negative-stranded templates for the viral RNA and mRNA's had been synthesized. Figure 1A shows the effect of increasing UV doses on the synthesis of virus-specific RNA during the 30 min after irradiation. Survival of 37%, corresponding to an average of one hit per RNA template, was reached at a UV dose of about 1,000 erg mm^{-2}. The nonlinearity of the dose-response curve indicates a multicomponent character of the template. A similar curve was obtained when the labeling was started at 6.6 h postinfection, the end of the labeling period in experiment 1, indicating that there was no repair in the first 0.5 h after UV irradiation (Fig. 1B).

The distribution of the label among the seven RNA species present in unirradiated virus-infected cells is shown in Table 1. RNA 1 and RNA 7 were the most abundant species, with the latter amounting to about one-half of the viral RNA, estimated on a molar basis. About 10^6 cpm of [^{3}H]uridine per tissue culture dish was incorporated into virus-specific RNA. This amount was sufficient to estimate the effect of UV irradiation on the individual RNAs, even for RNA 4, which contained only about 6% of the total label.

Effect of UV irradiation on the synthesis of the individual virus-specific RNAs. After extraction from infected cells, the individual

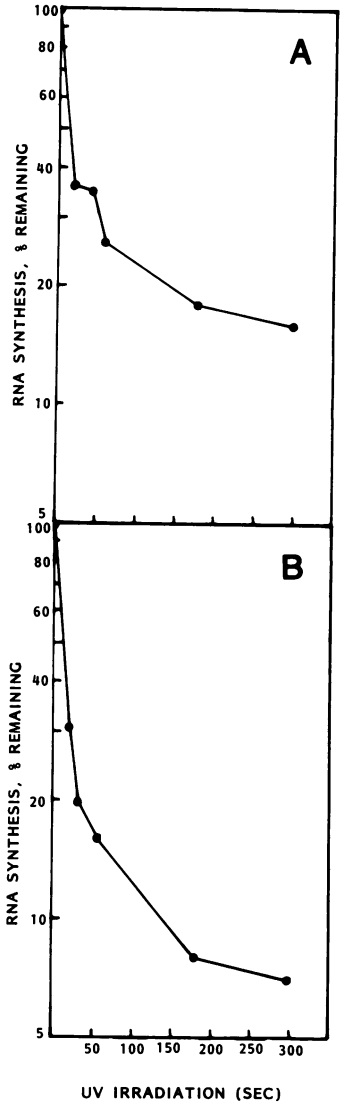

FIG. 1. *Effect of UV irradiation on the overall synthesis of virus-specific RNA in MHV-A59 infected Sac(−) cells. Actinomycin D-treated cells were irradiated with UV light at 6 h postinfection and then labeled in the presence of 1 μg of actinomycin D per ml with [^{3}H]uridine from (A) 6.1 to 6.6 h postinfection or (B) from 6.6 to 7.1 h postinfection. Background incorporation into uninfected cells (about 5% of the incorporation of the unirradiated control) was subtracted to calculate the remaining virus-specific RNA synthesis at the various UV doses.*

RNAs were separated by agarose gel electrophoresis. The resulting fluorograph (Fig. 2) shows that, in UV-irradiated cells, the normal set of RNAs is synthesized but in lesser amounts; the smaller the RNA, the more resistant to UV irradiation is its synthesis. To quantitate the amounts of RNA synthesized, bands were cut from the gel, and the gel slices were dissolved in scintillation fluid. The results of two representative experiments are shown in Fig. 3. Figure 3A shows the data for RNAs 1 to 5, in which RNA 4 and RNA 5 were processed together. The results for RNAs 6 and 7 are shown in Fig. 3B together with the individual values for RNA 4 and RNA 5. It is evident from Fig. 3 that the logarithms of the rate of continuing RNA synthesis [$\ln(N_t/N_0)$] are linearly correlated with the UV doses, a result which is to be expected if the Poisson distribution applies. Figure 3 also shows that the slope of the curve increases with the size of the RNA.

Numerical values for the slopes of the curves obtained by linear regression analysis were used

TABLE 1. *Relative abundance of virus-specific RNAs synthesized between 6.1 and 6.6 h postinfection in MHV-A59-infected Sac(−) cells*[a]

RNA	Mol wt (× 10^6)	cpm (%)	Relative molarity (%)
1	5.6	37.4	10.4
2	4.0	12.0	4.7
3	3.0	8.2	4.2
4	1.4	5.9	6.5
5	1.2	10.1	13.1
6	0.9	9.1	15.7
7	0.6	17.5	45.5

[a] [^{3}H]uridine-labeled, virus-specific RNA species were separated by agarose gel electrophoresis. The individual bands were excised from the gel and counted to determine the fraction of the label present in each RNA. The relative molarity of each RNA species was calculated.

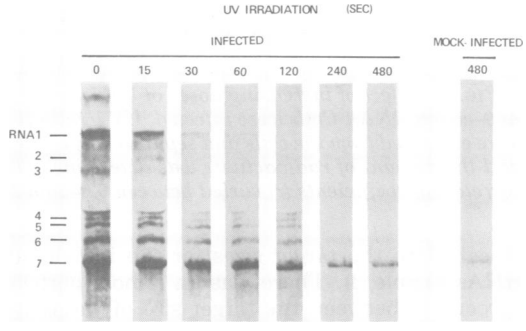

FIG. 2. *Agarose gel electrophoresis of the virus-specific RNAs synthesized between 6.1 and 6.6 h postinfection in MHV-A59-infected cells that were exposed to increasing doses of UV irradiation. The lanes contain RNA extracted from equal numbers of cells. Denatured nucleic acids were electrophoresed in a urea-containing gel and detected by fluorography. The positions of the seven virus-specific RNAs are indicated.*

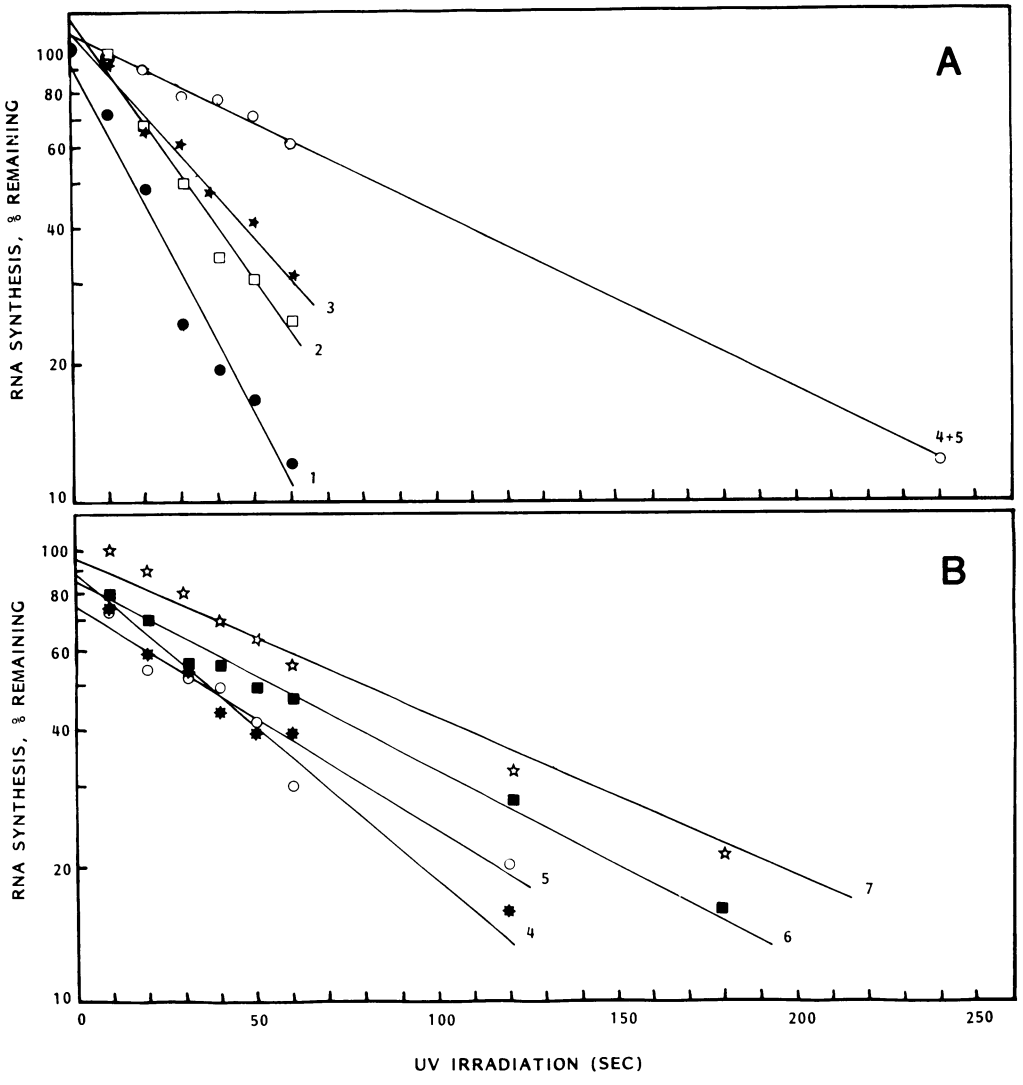

FIG. 3. *Effect of increasing doses of UV irradiation on the synthesis of the individual intracellular MHV-A59-coded RNAs. Cells were infected, UV irradiated, and labeled as described in the legend to Fig. 1. RNAs were extracted from the cells and separated by electrophoresis (Fig. 2); RNA bands were cut out and dissolved, and the amount of radioactivity was determined. The graphs were fitted by linear regression analysis. The correlation coefficients (r) varied between 0.94 and 1.00. (A) Experiment 1; (B) experiment 2.*

to calculate the target sizes for the individual RNAs (Table 2). There was an almost perfect agreement between the target size of the templates of RNAs 1 to 7 and the physical sizes of these RNAs as determined previously (7).

DISCUSSION

These data on the UV inactivation of the negative-stranded template for MHV-A59 genomic RNA and the subgenomic mRNA's present the first evidence that such a template exists in coronavirus-infected cells. Although isolation and characterization of the template are needed for a more detailed knowledge of the replication mechanism, the results at this point allow us to make a choice between two plausible transcription mechanisms. The first strategy would encompass the synthesis of full-length, positive-stranded RNA molecules, which are either processed by endonucleases or due to a splicing mechanism, to give rise to the six smaller RNAs. This alternative can be excluded since all RNAs then should have the same UV target size.

TABLE 2. *Comparison of the molecular weights of the MHV-A59 intracellular RNAs and the UV target sizes of their respective templates*

Expt	RNA	$K \times T^a$ (s^{-1})	Target size of template (mol wt $\times 10^6$)[b]	RNA size (mol wt $\times 10^6$)[c]
1	1	3.57×10^{-2}	5.6	5.6
	2	2.52×10^{-2}	3.9	4.0
	3	1.94×10^{-2}	3.0	3.0
	4 + 5	0.90×10^{-2}	1.4	1.2–1.4
2	4	1.44×10^{-2}	1.4	1.4
	5	1.28×10^{-2}	1.2	1.2
	6	1.00×10^{-2}	0.97	0.9
	7	0.77×10^{-2}	0.75	0.6

[a] $K \times T$ was calculated from the relationship $\ln(N_t/N_0) = -K \times T \times t$, where N_t represents the incorporation of [^{3}H]uridine into RNA after t seconds of UV irradiation; N_0 is the RNA synthesis in the unirradiated culture; T is the target size; and K is a constant. The calculation was made from the data points illustrated in Fig. 3 by using linear regression analysis. The value of K was calculated as 6.38×10^{-9} s^{-1} by substituting a value of 5.6×10^6 for the target size of RNA 1 (experiment 1) or 10.3×10^{-9} inserting a value of 1.4×10^6 for RNA 4 (experiment 2).

[b] By using the two values for K described in footnote *a* above, the target sizes for the other RNAs were calculated.

[c] The molecular weights of the denatured virus-specific RNAs were determined by agarose gel electrophoresis (7).

A UV target size of the template of the MHV-A59-specific RNAs which is identical to their physical size is consistent with the second strategy: an independently initiated transcription of each RNA on a genome-sized, negative-stranded template. A variant of this strategy, namely, independent transcription of a number of smaller templates, cannot be excluded, however, as long as the negative-stranded template has not been characterized.

Ultimately, determination of the nucleotide sequence of the negative-stranded RNA template will shed light on the sequence(s) recognized by the viral RNA polymerase. If all positive-stranded RNAs had the same 5'-terminal sequence, only one initiation site for the RNA polymerase would be needed. This could be accomplished in two ways. (i) The RNAs have a leader sequence. Our results exclude the possibility that such a sequence can arise by splicing from larger precursor molecules, but an RNA polymerase jump during transcription to 3'-proximal parts of the template could produce the same result. This would be an unprecedented mechanism, however, and its accuracy is difficult to imagine. (ii) Transcription of all RNAs starts at the 3' end of the genome-sized, negative-stranded template, and all RNAs have an identical 5'-terminal region of the size of RNA 7. For reasons published before (4, 7), it seems more likely that the genomic and subgenomic RNAs of MHV-A59 have a common 3'-terminal sequence; results obtained with an avian coronavirus (9) support this view.

If this assumption is correct, our findings would predict that sequences complementary to the promoter-initiator sites on the negative-stranded template are present on the genome at seven different positions, one for each of the seven RNAs. Differences at these sites might explain the divergent molar ratios among the RNAs. In this respect, it will be interesting to compare the transcription mechanisms of MHV-A59 and vesicular stomatitis virus. Results have been obtained which suggest that viral mRNA synthesis of vesicular stomatitis virus occurs by multiple initiations at different promoter sites (10). Vesicular stomatitis virus differs from MHV-A59, however, in that the elongation of the individual mRNA's is dependent on prior transcription of 3'-proximal genes. Another difference would be that mRNA synthesis of vesicular stomatitis virus terminates before the initiation site for the transcription of the next mRNA, whereas for MHV-A59, there would be a read-through until the 5' end of the template.

ACKNOWLEDGMENTS

We thank M. Maas Geesteranus and N. M. Oelp-Verhagen for the preparation of this manuscript.

LITERATURE CITED

1. **Laskey, R. A., and A. D. Mills.** 1975. Quantitative detection of ^{3}H and ^{14}C in polyacrylamide gels by fluorography. Eur. J. Biochem. **56**:335–341.
2. **McMaster, G. K., and G. G. Carmichael.** 1977. Analysis of single- and double-stranded nucleic acids on polyacrylamide and agarose gels by using glyoxal and acridine orange. Proc. Natl. Acad. Sci. U.S.A. **74**:4835–4838.
3. **Miller, R. L., and P. G. W. Plagemann.** 1974. Effect of ultraviolet light on mengovirus: formation of uracil dimers, instability and degradation of capsid, and covalent linkage of protein to viral RNA. J. Virol. **13**:729–739.
4. **Rottier, P. J. M., W. J. M. Spaan, M. C. Horzinek, and B. A. M. van der Zeijst.** 1981. Translation of three mouse hepatitis virus strain A59 subgenomic RNAs in *Xenopus laevis* oocytes. J. Virol. **38**:20–26.
5. **Sauerbier, W., and K. Hercules.** 1978. Gene and transcription unit mapping by radiation effects. Annu. Rev. Genet. **12**:329–363.
6. **Siddell, S. G., H. Wege, A. Barthel, and V. ter Meulen.** 1980. Coronavirus JHM: cell-free synthesis of structural protein p60. J. Virol. **33**:10–17.
7. **Spaan, W. J. M., P. J. M. Rottier, M. C. Horzinek, and B. A. M. van der Zeijst.** 1981. Isolation and identification of virus-specific mRNAs in cells infected with mouse hepatitis virus (MHV-A59). Virology **108**:424–434.

8. **Stern, D. F., and S. I. T. Kennedy.** 1980. Coronavirus multiplication strategy. I. Identification and characterization of virus-specified RNA. J. Virol. **34**:665–674.
9. **Stern, D. F., and S. I. T. Kennedy.** 1980. Coronavirus multiplication strategy. II. Mapping the avian infectious bronchitis virus intracellular RNA species to the genome. J. Virol. **36**:440–449.
10. **Testa, D., P. K. Chanda, and A. K. Banerjee.** 1980. Unique mode of transcription in vitro by vesicular stomatitis virus. Cell **21**:267–275.
11. **van der Zeijst, B. A. M., M. C. Horzinek, L. Jacobs, P. J. M. Rottier, and W. J. M. Spaan.** 1981. Messenger RNAs of mouse hepatitis virus A59: isolation and characterization, translation in *Xenopus laevis* oocytes of RNAs 3, 6 and 7, UV target sizes of the transcription templates. *In* V. ter Meulen, S. G. Siddell, and H. Wege (ed.), Biochemistry and biology of coronaviruses. Plenum Publishing Co., London.